The Astrophysical Journal Letters, 836:L20 (4pp), 2017 February 20 https://doi.org/10.3847/2041-8213/aa5eb0

H_2O Megamasers toward Radio-bright Seyfert 2 Nuclei*

J. S. Zhang[1], Z. W. Liu[1], C. Henkel[2,3], J. Z. Wang[4], and G. V. Coldwell[5]
[1] Center for Astrophysics, Guangzhou University, Guangzhou, 510006, China; jszhang@gzhu.edu.cn
[2] Max-Planck-Institut für Radioastronomie, Auf dem Hügel 69, D-53121 Bonn, Germany
[3] Astronomy Department, King Abdulaziz University, P.O. Box 80203, Jeddah 21589, Saudi Arabia
[4] Shanghai Astronomical Observatory, Chinese Academy of Sciences, 80 Nandan Road, Shanghai 200030, China
[5] FCEFyN-UNSJ-CONICET, San Juan, Argentina
Received 2016 December 31; revised 2017 January 27; accepted 2017 February 6; published 2017 February 16

Abstract

Using the Effelsberg-100 m telescope, we perform a successful pilot survey on H_2O maser emission toward a small sample of radio-bright Seyfert 2 galaxies with a redshift larger than 0.04. The targets were selected from a large Seyfert 2 sample derived from the spectroscopic Sloan Digital Sky Survey Data Release 7 (SDSS-DR7). One source, SDSS J102802.9+104630.4 ($z \sim 0.0448$), was detected four times during our observations, with a typical maser flux density of ∼30 mJy and a corresponding (very large) luminosity of $\sim 1135\, L_\odot$. The successful detection of this radio-bright Seyfert 2 and an additional tentative detection support our previous statistical results that H_2O megamasers tend to arise from Seyfert 2 galaxies with large radio luminosity. The finding provides further motivation for an upcoming larger H_2O megamaser survey toward Seyfert 2s with particularly radio-bright nuclei with the basic goal to improve our understanding of the nuclear environment of active megamaser host galaxies.

Key words: galaxies: active – galaxies: nuclei – galaxies: Seyfert – masers – radio continuum: galaxies

1. Introduction

Extremely luminous masers in the $J_{K_aK_c} = 6_{16} - 5_{23}$ line (rest frequency of 22.23508 GHz) with an isotropic luminosity no less then $10\, L_\odot$ are termed "megamasers" and are mostly detected in heavily obscured type-2 active galactic nuclei (AGNs; e.g., Braatz et al. 1997; Zhang et al. 2006, 2010; Greenhill et al. 2008). These H_2O megamasers have become a valuable tool for investigating a series of key astrophysical issues, e.g., estimating the mass of supermassive black holes (SBHs); probing the physics, morphology, and kinematics of accretion disks or tori; constraining the black hole–bulge mass relation (Miyoshi et al. 1995; Morganti et al. 2004; Greene et al. 2010; Kuo et al. 2011; Pesce et al. 2015; Läsker et al. 2016); and providing a perspective to improve the accuracy of the Hubble constant and to constrain the equation of state for the elusive dark energy (e.g., Reid et al. 2013). Adequate numbers of H_2O megamasers, especially "disk masers" (its maser spots can be modeled by an edge-on Keplerian disk surrounding the central engine; maser spectral features include systemic velocity and redshifted and blueshifted high-velocity components), are obviously required to and valuable for tackling these key issues. However, the detection rate of H_2O megamasers is quite low so far (e.g., Greenhill et al. 2003; Henkel et al. 2005; Kondratko et al. 2006; Zhang et al. 2006; Braatz & Gugliucci 2008; Bennert et al. 2009; König et al. 2012; Wagner 2013; Wiggins et al. 2016). For nearly 40 years (Churchwell et al. 1977), 22 GHz H_2O maser emission was detected in merely ∼160 among over 4000 targeted galaxies (Megamaser Cosmology Project (MCP) webpage[6]), with an average detection rate of ∼4%.

Maser emission appears to depend on the nuclear radio power, which was supported by statistical analysis on radio data of maser host Seyfert 2s and non-masing Seyfert 2s (Braatz et al. 1997; Zhang et al. 2012). Based on archival data from different telescopes, it shows that maser Seyfert 2s have higher nuclear radio luminosities than non-masing Seyfert 2s, and nuclear radio luminosity was supposed to be a suitable indicator to guide future AGN maser searches (Zhang et al. 2012). This has been confirmed by our follow-up study on multi-band (11, 6, 3.6, 2, 1.3 cm) radio properties of maser host Seyfert 2s, through systematic Effelsberg observations (Liu et al. 2017).

Thus, we performed a pilot survey with the Effelsberg-100 m telescope, searching for new H_2O megamasers toward a small sample of Seyfert 2s with radio-bright nuclei. Our targets including 18 sources were selected from a large Seyfert 2 sample containing 4035 sources, which was derived from the SDSS-DR7 covering a redshift range from 0.04 to 0.1 (Coldwell et al. 2013). Those selected 18 Seyfert 2s are relative nearby ($z < 0.05$) with decl. $\delta > -20°$ and have high radio luminosity at 20 cm (data from the NRAO VLA Sky Survey catalog, http://www.cv.nrao.edu/nvss/, with a threshold of 10^{29} erg s^{-1} Hz^{-1}; Liu et al. 2017), which have not searched for H_2O maser emission before according to the H_2O maser survey catalog from the MCP webpage (see the second footnote). In Section 2, we describe our observations and data reduction. We present the main results and corresponding discussions in Section 3. A brief summary including future prospects is given in Section 4.

2. Observations and Data Reduction

We performed our observations on radio K-band H_2O megamasers searching between 2016 January 28 and February 1, making use of the Effelsberg-100 m telescope. The secondary focus receiver S14MM01 (18.5–22.235 GHz) was used with an XFFT spectrometer encompassing 500 MHz and 65,536 channels. It provides a channel spacing of ∼7.2 kHz, which corresponds to a velocity width of ∼0.10 km s^{-1}. The center frequency was set to 21.25 GHz, according to the redshift range of our sample. The observations were obtained in

* Based on observations with the 100 m telescope of the MPIfR (Max-Planck-Institut für Radioastronomie) at Effelsberg.
[6] https://safe.nrao.edu/wiki/bin/view/Main/PrivateWaterMaserList

Table 1
H_2O Maser Pilot Survey toward a Small Sample of Radio-bright Seyfert 2s from the SDSS-DR7

Source	R.A. (*J* 2000)	Decl.	V_{sys} (*cz*)	$F_{20\,cm}$ (mJy)	Time (minutes)	rms (mJy)
SDSS J080047.66+374343.3	08:00:47.22	+37:43:48.1	12489	10.2	42	12.2
SDSS J090822.15+320646.6	09:08:22.29	+32:06:46.6	14883	4.3	40	11.8
SDSS J092329.29+254608.7	09:23:28.93	+25:46:07.7	14937	4.5	39	12.3
SDSS J093141.45+474209.0	09:31:41.45	+47:42:09.09	14574	6.8	40	17.7
SDSS J100135.80+033647.8	10:01:35.94	+03:36:47.6	12798	3.7	40	13.8
SDSS J102802.88+104630.4	10:28:02.86	+10:46:31.2	13424	2.4	171	7.33
SDSS J103328.10+162251.0	10:33:28.12	+16:22:53.7	13518	13.8	40	12.9
SDSS J123019.40+032712.7	12:30:19.58	+03:27:11.5	14610	3.8	39	14.5
SDSS J123838.10+453414.4	12:38:38.10	+45:34:14.47	12138	7.4	12	31.6
SDSS J130422.19+361543.1	13:04:22.47	+36:15:42.5	13278	9.0	36	13.8
SDSS J134736.39+173404.6	13:47:36.39	+17:34: 5.7	13398	13	39	14.4
SDSS J144921.58+631614.0	14:49:21.74	+63:16:13.9	12471	3006	15	30.9
SDSS J145448.62+003828.8	14:54:48.81	+00:38:30.2	13038	8.0	76	8.7
SDSS J150126.33+020410.8	15:01:26.52	+02:04:11.2	12702	2.2	46	15.2
SDSS J160153.01+452107.0	16:01:53.64	+45:21:07.1	12600	2.2	31	21.5
SDSS J160445.00+444316.9	16:04:44.68	+44:43:15.9	12999	3.2	20	26.4
SDSS J161735.00+501440.4	16:17:35.09	+50:14:39.8	12420	8.7	40	18.8
SDSS J162631.28+260016.2	16:26:31.10	+26:00:16.6	14745	2.6	40	16.9

Note. Coordinates were taken from NED (NASA/IPAC Extragalactic Database). $F_{20\,cm}$ is the radio flux density at 20 cm in mJy from the NRAO VLA Sky Survey (NVSS) catalog, and rms (mJy) for each source is derived from the baseline fit of its spectra at the original velocity resolution (see Section 2). Time represents the total integration time, including on + off time. The sources in bold style and italic style represent the new detection and one tentative detection, respectively.

a position switching mode, with the off-position offset by 900 arcsec in R.A. Signals from individual on- and off-source positions were integrated for 120 s each, and 10 repeats give a typical on-source integration time of ~20 minutes. System temperatures were about 55–85 K on a main beam brightness temperature scale. Pointing was checked about each hour, while the focus was corrected roughly every 2 ~ 3 hr, using nearby calibrators (Baars et al. 1977; Ott et al. 1994). The Gildas software package (e.g., Guilloteau & Lucas 2000) was used for our data reduction.

Calibration was obtained by measuring the calibrator source 3C 286. Based on its flux density of 2.54 Jy at 21.250 GHz (Ott et al. 1994) and an average amplitude of 0.172 in units of the flux of the employed noise diode and an average telescope gain of 0.95 of the source during our observations, we obtain a calibration factor of 2.54/(0.172/0.95) ~14, with an estimated uncertainty of 15%.

Our observations of the 18 radio-bright Seyfert 2s are listed in Table 1, including the radio flux density at 20 cm from the NRAO VLA Sky Survey (NVSS; Condon et al. 2002), the total integration time (on + off time), and estimated rms values from baseline fitting of each source at the original velocity width of ~0.10 km s^{-1}.

3. Results and Discussion

Among our pilot survey sample of radio-bright Seyfert 2s listed in Table 1, one source (SDSS 102802.9+104630.4) was repeatedly found to exhibit emission (see the following details). Another source (SDSS J093141.4+474209) may represent a tentative detection.

SDSS 102802.9+104630.4: During all four scheduled observing periods, H_2O megamaser emission was detected toward this Seyfert 2 galaxy ($V_{LSR,optical}$ ~ 13424 km s^{-1}, $z \sim 0.044776$, $D_L \sim 195$ Mpc; Stein 1996; Catinella et al. 2013). All spectra (upper four panels in Figure 1) show a similar amplitude and line shape within the error limits. Only linear (order 1) polynomials had to be subtracted to get good baselines within a few 100 km s^{-1} on each side of the profiles. The elevations were 50°, 40°, 32°, and 50° during the four periods of observations. After considering the gain correction due to these different elevations, the calibration factors become 14.31, 14.00, 14.00, and 14.31, respectively. The average spectrum is shown in Figure 1 (bottom panel; with a velocity resolution of ~7.20 km s^{-1}), and its fitting gives a line width of 45.4 ± 2.1 km s^{-1}, a line-center velocity of −22.6 ± 0.9 with respect to the systemic velocity (see Table 1), and a peak intensity of ~26.9 mJy. The integrated flux density is 1297.5 ± 50.9 mJy km s^{-1}, which yields a corresponding isotropic luminosity of ~1135 $L_\odot$ ($L_{H_2O}/[L_\odot] = 0.023 \times \int S\, dV/[\mathrm{Jy\,km\,s^{-1}}] \times D^2[\mathrm{Mpc}^2]$), so that the source hosts one of the most luminous H_2O megamasers ever detected.

SDSS J093141.4+474209: This source ($V_{LSR,optical}$ ~14,580 km s^{-1}, $z \sim 0.048635$, $D_L \sim 200$ Mpc, 2004SDSS2[7]) was observed on January 29, with an integration time (on + off) of 40 minutes. Figure 2 shows its average spectra, with a channel width smoothed to 1.1 km s^{-1}. The fitting leads to a line width of of 8.9 ± 1.0 km s^{-1}, a line-center velocity of 148.2 ± 0.5 with respect to the velocity value in Table 1, a peak intensity of ~43.5 mJy and an integrated flux density of 409.9 ± 45.4 mJy km s^{-1}, which gives a corresponding isotropic luminosity of ~377 $L_\odot$. The signal-to-noise-ratio is ~7, but we prefer to be cautious and only take this as a tentative detection (errors are merely formal values), because of some evidence for the presence of weak ripples in the spectrum.

Our pilot survey is quite successful in selecting H_2O megamaser candidates compared to previous observations, though the detection rate is still not very high, with 5.5% or 11% (1 or 2 out of 18). We note, however, that our galaxies are $0.04 < z < 0.05$ farther away than most targets of other surveys and that therefore only very luminous sources are

[7] http://www.sdss.org/dr2/products/spectra/getspectra.html

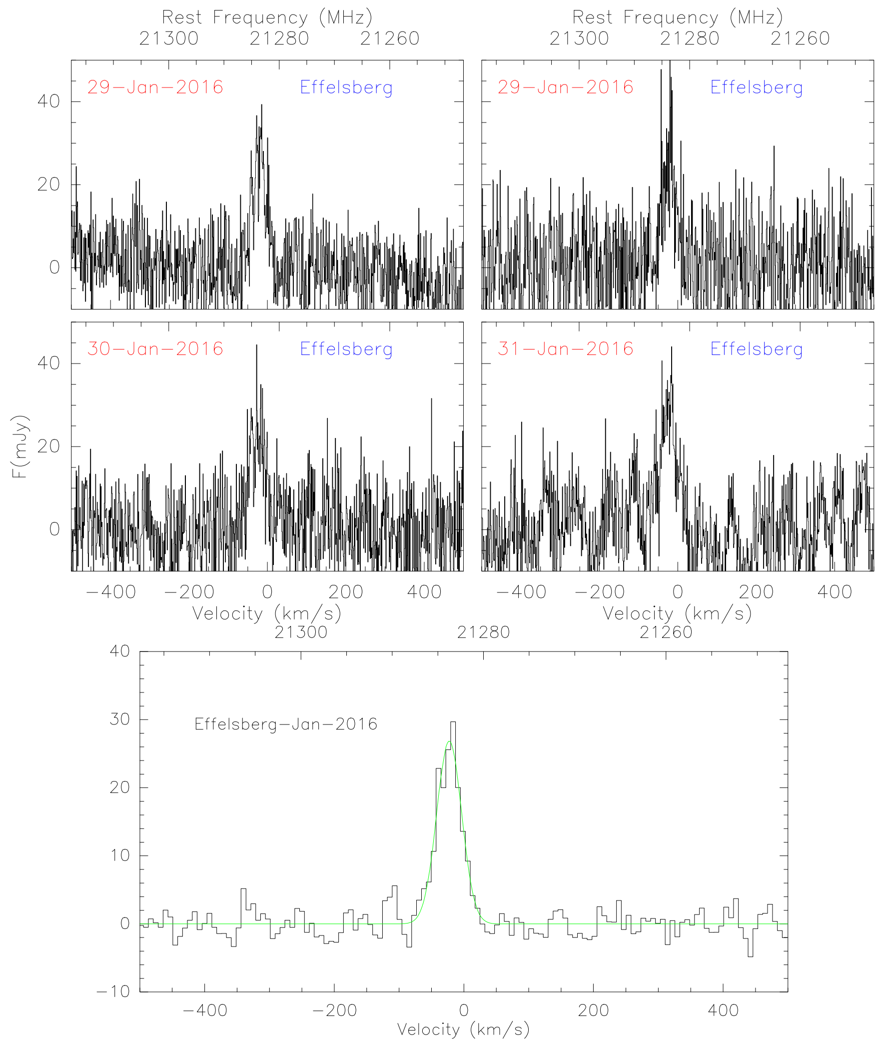

Figure 1. Spectra at each period (upper panels) and the smoothed average spectra with the fitting line (lower panel) of the new megamaser source SDSS 102802.9 +104630.4, with a redshift of 0.044776. The velocity scale refers to the NED velocity given in Table 1.

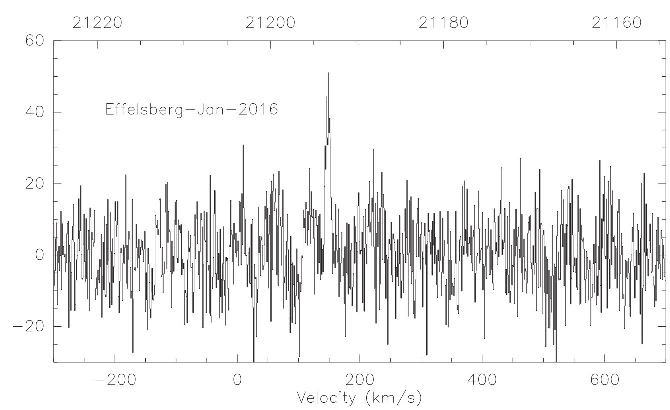

Figure 2. Average spectrum of SDSS J093141.4+474209 ($z \sim 0.048635$) is presented, with a velocity resolution of 1.1 km s^{-1}. The velocity scale refers to the NED velocity given in Table 1.

above the detection threshold. In this regard, our detection rate, although based on only a few sources, appears to be quite high. The successful detection of H_2O megamasers toward Seyfert 2s with bright radio nuclei supports our previous proposition that H_2O megamasers tend to locate in radio-bright Seyfert 2s, which was derived from our statistical analysis on both archival radio data (Zhang et al. 2012) and systematic observations by the Effelsberg telescope (Liu et al. 2017).

A part of the H_2O nuclear maser emission may be caused by the amplification of the nuclear radio emission, which provides "seed" photons for the circumnuclear maser clouds located on the front side of the nuclear radio source along our sightline. These "seeds" from nuclear continuum radiation could be amplified by the foreground maser clouds (Braatz et al. 1997; Henkel et al. 1998; Herrnstein et al. 1998; Lo 2005). However, in the standard picture of disk masers, only the systemic features should amplify seed photons, while the blueshifted and redshifted high-velocity emission would not profit from this effect, thus remaining difficult to detect. We note that the majority of the best and strongest disk maser systems discovered by the MCP so far are systems in which the masers mostly likely amplify their own spontaneous emission (no continuum was detected on the milliarcsecond scales). On the other hand, the radio luminosity may be taken as a good isotropic tracer of AGN activity (Giuricin et al. 1990; Diamond-Stanic et al. 2009). A strong AGN may hint at active accretion and jet formation (Braatz et al. 1997) and a large amount of gas in the nuclear environment. This is corroborated by our statistical result that the accretion rates of maser Seyfert

2s are nearly one order larger than non-masing Seyfert 2s (Liu et al. 2017).

Given the fact that H_2O megamasers are associated with radio-bright Seyfert 2s from our previous statistical results and the pilot survey, the radio luminosity of Seyfert 2s provides a suitable indicator to guide future H_2O megamaser searches toward large Seyfert 2 samples, e.g., toward the radio-bright part of the Seyfert 2 sample of 4035 targets from the SDSS-DR7 release. More H_2O megamaser detections at large distance (redshift >0.04; to date, almost all known H_2O megamaser sources have a redshift less than 0.04) are expected toward big samples with such radio-bright Seyfert 2 nuclei. Finding a large number of such sources at a large distance will help us to improve our understanding of the enigmatic highly obscured nuclear regions of active galaxies.

4. Summary

Based on our statistical analysis on both archival radio data (Zhang et al. 2012) and systematic observations by the Effelsberg telescope (Liu et al. 2017), H_2O megamasers tend to locate in radio-bright Seyfert 2s. Thus, we selected one small radio-bright Seyfert 2 sample, not having been searched for H_2O maser before, to perform a pilot survey on H_2O megamaser emission. Our survey led to one new megamaser source and one additional possible detection, which reflects our success in selecting H_2O megamaser candidates compared to previous observations. While our detection rate of 5.5% or 11% (the latter including a tentative detection) appears to be higher than in most other surveys (the uncertainty lies in the limited number of studied sources), the distance to our targets is also larger, thus making the success of this pilot survey particularly noteworthy. The new megamaser (SDSS 102802.9+104630.4) source is one of the strongest megamasers published to date, with an isotropic luminosity larger than $1000\,L_{\odot}$. Our successful selection technique may provide good guiding for future H_2O megamaser surveys, i.e., Seyfert 2s with radio-bright nuclei. More H_2O detections at a large distance (redshift >0.04) can be expected from a large systematic survey of such radio-bright Seyfert 2 galaxies. These have the great potential to increase our knowledge on the central highly obscured but still very enigmatic regions of active Seyfert galaxies.

This work is supported by the Natural Science Foundation of China (No. 11473007, 11590782). We thank the staff at the Effelsberg-100 m for their kind help during our observations. We have made use of the NASA/IPAC Extragalactic Database (NED), which is operated by the Jet Propulsion Laboratory, California Institute of Technology, under contract with the National Aeronautics and Space Administration.

References

Baars, J. W. M., Genzel, R., Pauliny-Toth, I. I. K., & Witzel, A. 1977, A&A, 61, 99
Bennert, N., Barvainis, R., Henkel, C., & Antonucci, R. 2009, ApJ, 695, 276
Braatz, J. A., & Gugliucci, N. E. 2008, ApJ, 678, 96
Braatz, J. A., Wilson, A. S., & Henkel, C. 1997, ApJS, 110, 321
Catinella, B., Schiminovich, D., Cortese, L., et al. 2013, MNRAS, 436, 34
Churchwell, E., Witzel, A., Huchtmeier, W., et al. 1977, A&A, 54, 969
Coldwell, G. V., Gurovich, S., & Díaz, T. J. 2013, MNRAS, 437, 1199
Condon, J. J., Cotton, W. D., & Broderick, J. J. 2002, AJ, 124, 675
Diamond-Stanic, A. M., Rieke, G. H., & Rigby, J. R. 2009, ApJ, 698, 623
Giuricin, G., Mardirossian, F., Mezzetti, M., & Bertotti, G. 1990, ApJS, 72, 551
Greene, J. E., Peng, C. Y., Lo, K. Y., Henkel, C., & Reid, M. 2010, ApJ, 721, 26
Greenhill, L. J., Kondratko, P. T., Lovell, J. E. J., et al. 2003, ApJL, 582, L11
Greenhill, L. J., Tilak, A., & Madejski, G. 2008, ApJL, 686, L13
Guilloteau, S., & Lucas, R. 2000, in ASP Conf. Ser. 217, Imaging at Radio through Submillimeter Wavelengths, ed. J. G. Mangum & S. J. E. Radford (San Francisco, CA: ASP), 299
Henkel, C., Peck, A. B., Tarchi, A., et al. 2005, A&A, 436, 75
Henkel, C., Wang, Y. P., Falcke, H., Wilson, A. S., & Braatz, J. A. 1998, A&A, 335, 463
Herrnstein, J. R., Greenhill, L. J., Moran, J. M., et al. 1998, ApJL, 497, L69
Kondratko, P. T., Greenhill, L. J., & Moran, J. M. 2006, ApJ, 652, 136
König, S., Eckart, A., Henkel, C., & Garcia-Marin, M. 2012, MNRAS, 420, 2263
Kuo, C. Y., Braatz, J. A., Condon, J. J., et al. 2011, ApJ, 727, 20
Läsker, R., Greene, J. E., Seth, A., et al. 2016, ApJ, 825, 3
Liu, Z. W., Zhang, J. S., Henkel, C., et al. 2017, MNRAS, 466, 1608
Lo, K. Y. 2005, ARA&A, 43, 625
Miyoshi, M., Moran, J., Herrnstein, J., et al. 1995, Natur, 373, 127
Morganti, R., Greenhill, L. J., Peck, A. B., Jones, D. L., & Henkel, C. 2004, NewAR, 48, 1195
Ott, M., Witzel, A., Quirrenbach, A., et al. 1994, A&A, 284, 331
Pesce, D. W., Braatz, J. A., Condon, J. J., et al. 2015, ApJ, 810, 65
Reid, M. J., Braatz, J. A., Condon, J. J., et al. 2013, ApJ, 767, 154
Stein, P. 1996, A&AS, 116, 203
Wagner, J. 2013, A&A, 560, 12
Wiggins, B. K., Migenes, V., & Smidt, J. M. 2016, ApJ, 816, 55
Zhang, J. S., Henkel, C., Guo, Q., Wang, H. G., & Fan, J. H. 2010, ApJ, 708, 1528
Zhang, J. S., Henkel, C., Kadler, M., et al. 2006, A&A, 450, 933
Zhang, J. S., Henkel, C., Wang, J., & Guo, Q. 2012, A&A, 538, 152